Nuclear data uncertainties propagation and quantification analysis on the PWR core level based on generalized perturbation theory

HAO Chen[1,*], MA Ji[1], ZHAO Qiang[1], ZHANG Huiyan[1], and CHEN Jianqiang[1]

1. *Fundamental Science on Nuclear Safety and Simulation Technology Laboratory, College of Nuclear Science and Technology, Harbin Engineering University, Harbin, China*

Abstract: Based on the idea of uncertainty propagation, the uncertainties of core parameters, such as k_{eff}, are propagated from few-group homogenized cross-sections in the traditional two-step neutronics calculation strategy. The generalized perturbation theory can be used to quantify and propagate nuclear data uncertainty in the whole core diffusion calculation. In order to use generalized perturbation theory two key technical problems, sensitivity coefficients to few-group cross- sections and the method of generating few-group cross-section-covariance matrices, should be considered reasonably. In this paper, k_{eff} sensitivity coefficients to few-group cross-sections has been derived by using generalized perturbation theory. And most notably, a method of correlation analysis between different few-group XSs based on sensitivity information has been studied in depth to generate few-group cross-section-covariance matrices for uncertainty analysis on the core level. The sensitivity and uncertainty analysis method have been verified respectively. Numerical results for AP1000 core at hot zero power and hot full power condition are also presented in this paper and the results support that the methods studied in this work can be used to conduct sensitivity and uncertainty analysis for nuclear cross sections on the core level.

Keywords: generalized perturbation theory; covariance matrix; correlation; uncertainty; sensitivity

1 Introduction

In recent years there has been an increasing demand from nuclear research, industry, safety and regulation for best estimation plus uncertainty analysis to be provided with their confidence bounds [1], rather than safety analysis with conservative assumption. In nuclear reactor physics calculations, there are three main uncertain sources:(i)nuclear data; (ii)engineering uncertainties, such as manufacturing tolerance of fuel and uncertainty in material composition;(iii) models and numerical calculation methods. With regard to models and numerical calculation methods, high-fidelity, first-principled based simulation of the multi-physics phenomena occurring in nuclear reactor and elaborated models can be exploited to reduce uncertainties [2]. However, uncertainties inevitably exist in nuclear data due to errors with the measurements and errors in the statistics data, which are represented in the form of multi-group covariance matrix and difficult to be eliminated only by upgrading the accuracy of experimental equipment. Consequently, sensitivity and uncertainty (SAU) method should be applied to quantify uncertainties of operation and safety core design parameters propagated from nuclear data.

The nuclear reactor physics calculation is complex and involves many calculation steps from the cross section (XS) database, such as the neutron energy spectrum, resonance self-shielding, cell, assembly, whole core and

Received date: June 29, 2017

burnup calculation. A popular and practical idea is to subdivide the complex calculation flow or system into several steps and identify the input, output and propagated uncertain parameters through in-depth study in each step by applying mechanism analysis or statistics analysis method. Today, for SAU analysis most notably are the project for the uncertainty analysis for modeling of Light Water Reactor (LWR) supported by OECD [1] and the IAEA CRP project for uncertainty analysis of High Temperature Gas Cooled Reactor (HTGR) [3]. In previous studies, many efforts were put on the study of SAU methods, code development [7-9] and SAU analysis on the cell and lattice level, which focused on the derivation of the multi-group XSs and few-group XSs and their uncertainties [4-6]. As a follow-up study, this paper presents an application of generalized perturbation theory (GPT) as a way to quantify the uncertainty of the core design parameter, k_{eff}, of the advanced commercial power reactor, AP1000, propagated from those buried in few-group XSs.

As for quantifying uncertainties of core parameters caused by those of nuclear data, two calculation schemes already exist. The first scheme is commonly referred to the direct one-step calculation (DOC) scheme, which directly propagates uncertainties in multi-group microscopic XSs to the core parameters. The TSUNAMI-3D (Tools for Sensitivity and Uncertainty Analysis Methodology Implementation in Three Dimensions) module is representative of this scheme, which provides for calculation of forward and adjoint neutron transport solutions by applying Monto Carlo (MC) method and for now only calculation of sensitivity coefficients and uncertainty in k_{eff} due to cross-section-covariance data by applying GPT [10]. Another popular and practical scheme is hybrid calculation (HC) scheme, *e.g.* utilizing GPT method in the lattice physics analysis phase and stochastic sampling (SS) method in the core level [11] or MC method in the first phase and also SS method in the second step [12]. At the same time, nuclear data uncertainties can be directly perturbed by applying XSUSA [13] to generate N sets of multi-group XS libraries, which are then respectively passed to a lattice physics transport solver to produce N perturbed, homogenized, few-group XS libraries. The perturbed few-group libraries are then used as uncertain inputs for core simulator. SS method is the only option for uncertainty quantification of core parameters in the above-mentioned references. Although uncertainties of some distribution parameters, such as power distributions, due to nuclear data uncertainties can be only quantified by SS method rather than GPT method, generating sample space from few-group XS covariance matrices inevitably introduces new uncertainties. At the same time, determination of a reasonable number of samples to obtain the desired statistical accuracy with a certain confidence level also should be studied in-depth. Even more important, sensitivity information cannot be directly obtained by applying SS method, especially the region-related sensitivity information. The sensitivity information of k_{eff} to few-group XSs in different regions of reactor core is the basic information and important for correlation analysis of k_{eff} under different core conditions, *e.g.* the process of lifting controls rods. An effective approach to quantify uncertainty of k_{eff} and sensitivity information to few-group XSs on the core level is GPT method.

In this work the sensitivities of k_{eff} to different few-group XSs are calculated by using generalized perturbation theory based on 3D neutron diffusion equation, the details of which are provided in section 3.1. Another key problem is how to determine the covariance between different few-group XSs chosen from all the possible parings of fuel assembly types comprising the core. To do so, the SCALE6.1

module TSUNAMI-2D [14] is used to generate uncertainties of few-group XSs and sensitivity information of those to multi-group XSs. Based on these sensitivity information, an extended method of correlation analysis between different few-group XSs is studied in-depth, the details of which are provided in section 4. Then the correlation information between different few-group XSs combined with their uncertainty information leads one to construct the global covariance matrix. Based on the method studied in this paper, a Perturbation Theory Module for Uncertainty and Sensitivity analysis (PETMUS) has been developed and successfully coupled with the core simulator CITATION [15,16] to quantify the uncertainty of core k_{eff} propagated from few-group XSs and related sensitivity information for now. At last, uncertainties of k_{eff} of the traditional first core of the advanced commercial power reactor AP1000 at the hot zero power (HZP) state and hot full power (HFP) state has been quantified and the related sensitivity to few-group XSs has also been obtained.

2 Description of the core model

2.1 Simplified AP1000 traditional first core model

The uncertainty analysis has been applied to the simplified AP1000 traditional first core, where the first cycle core has a loading pattern of 157 fuel assemblies (FA), with the highest enrichment fuel on the core periphery and two other lower enrichments in the core interior. A set of 24 different assemblies are considered for the neutron transport lattice calculation according to the enrichment (2.35, 3.4, 4.45w/o), burnable absorbers (IFBA/Pyrex), control rod and axial heterogeneities of IFBA/Pyrex. All FAs have the same configuration, 17×17 with 24 guide thimbles and 1 instrumentation thimble at the center. The traditional first core (1/4) loading pattern of AP1000 with some gray and black M control banks (M-Banks) inserted fully into the core and without the axial offset (AO-Bank) control bank and SD Banks is shown in Fig.1. More detailed information for all the sets of FAs is given in Table 1. In this work, the whole core model altogether needs 628 FAs due to the axial heterogeneities of burnable absorbers.

Fig.1. Traditional first core(1/4) loading pattern of AP1000.

Table 1 Different types of assemblies in AP1000 traditional first core

	Assembly	Number of Assembly	^{235}U Enrichment (w/0)	Number of BPR (IFBA/Pyrex)	Control Rod Black/Gray
1	A1-000	37*4	2.35	0/0	--
2	A1-028	4*2	2.35	28/0	--
3	B1-028	12	3.40	28/24	--
4	B1-044	8	3.40	44/24	--
5	B1-088	32	3.40	88/24	--
6	C1-072	8	4.45	72/24	--
7	C1-088-09	8	4.45	88/9	--
8	C1-088-012	8	4.45	88/12	--
9	C1-112	32*2	4.45	112/0	--
10	C1-088-09M	8	4.45	88/0	--
11	C1-088-12M	8	4.45	88/0	--
12	A1-000B	8*4	2.35	0/0	Ag-In-Cd/SS
13	C1-072M	8	4.45	72/0	--
14	A1-028A	4*2	2.35	0/0	--
15	B1-028A	12*2	3.40	0/0	--
16	B1-044A	8*2	3.40	0/0	--
17	B1-088A	32*2	3.40	0/0	--
18	C1-088-09A	8*2	4.45	0/0	--
19	C1-088-12A	8*2	4.45	0/0	--
20	C1-072A	8*2	4.45	0/0	--
21	C1-112A	32*2	4.45	0/0	--
22	B1-028M	12	3.40	28/0	--
23	B1-044M	8	3.40	44/0	--
24	B1-088M	32	3.40	88/0	--

2.2 Mini-core model for verification

In order to effectively assess the credibility of k_{eff} uncertainty quantified by the method proposed in this work, an appropriate 3-D mini-core with using the typical AP1000 assemblies and reflective boundary conditions should be designed. The AP1000 mini-core configuration with the height of 320 cm and width of 64.26 cm is arranged in a 3×3 checkerboard pattern directly from the center of the AP1000 first core loading pattern, as shown in Fig.2. In this model, a set of 3 different FAs are considered according to the enrichment (2.1, 3.1w/o), burnable absorbers (Pyrex) and control rod. The FA configuration is same as those used in the AP1000 core and only difference is ^{235}U enrichment and the number of burnable absorbers. Region-2.1-RCCA is represented by the 2.1% enrichment with center Rod Cluster Control Assembly (RCCA) and Region-3.1-20PY is the 3.1% enriched region with the 20 Pyrex rods. The fuel is at beginning -of-life (BOF) and Hot Zero Power (HZP) isothermal conditions and the materials of control rod is B4C. At the same time, some simplifications have also been made in the mini-core for reducing the uncertainty introduced by models, such as removing the axial heterogeneities of burnable absorbers.

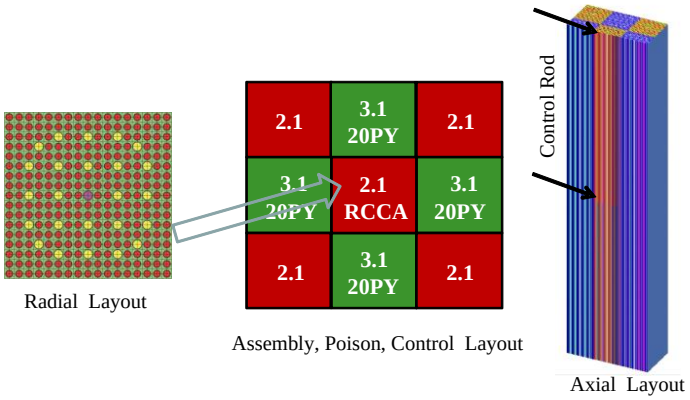

Fig. 2 AP1000 mini-core configurations.

2.3 Codes used for uncertainty analysis

In this study, the Tsunami-2D module in Scale 6.1, which is a comprehensive modeling and simulation suite for nuclear safety analysis and design, is used to propagate the uncertainty in nuclear data to the few-group macroscopic XSs of all the FAs and obtain the associated sensitivity information to the multi-group microscopic XSs. Based on these information, the few-group macroscopic XS covariance matrix on the full core level can be constructed. The Tsunami-2D module uses an original ENDF/B-VII.0 library in 238 energy groups. At the same time, the Scale 6.0 covariance library data in 44 energy groups [1], which corresponds to relative uncertainties assembled from a variety of sources, including evaluations from ENDF/B-VII, ENDF/B-VI, JENDL-3.3, and more than 300 approximated uncertainties from a collaborative project performed by Brookhaven National Laboratory (BNL), Los Alamos National Laboratory (LANL), and Oak Ridge National Laboratory (ORNL), is used to represent uncertainty in nuclear data.

The 3D diffusion calculation code CITATION used for this study is an enhanced version, which implements a finite-difference scheme for coarse-mesh few group diffusion calculation modified by Assembly Discontinuous Factor (ADF). The ADFs in the X-Y directions are provided by the NEWT module in Scale 6.1. Through 3D whole core diffusion calculation the flux and ad joint flux distribution on the full core can be calculated, which are important inputs to quantify the core k_{eff} sensitivity information to the few-group macroscopic XSs based on generalized perturbation theory. The PETMUS code developed for this study is applied to calculate k_{eff} sensitivity coefficients to the macroscopic XSs and quantify the uncertainty of k_{eff} propagated from nuclear data. A scheme of quantifying k_{eff} uncertainty is shown in Fig. 3.

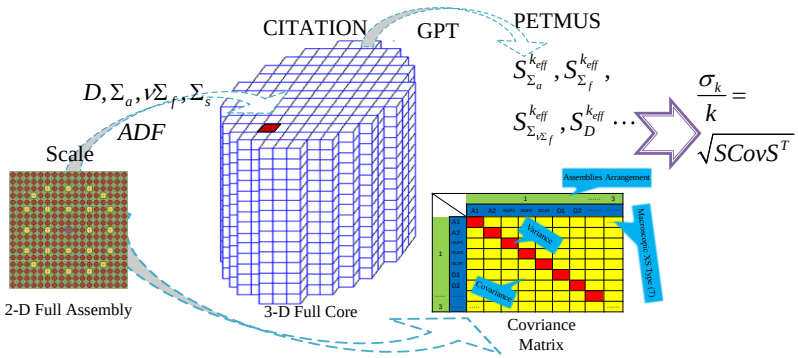

Fig. 3 Scheme of AP1000 core k_{eff} uncertainty analysis.

3 k_{eff} sensitivity coefficient to macroscopic XSs based on GPT and diffusion theory

The sensitivity coefficient is a measure of the change in a response R due to the variation of the estimated parameter. The response R sensitivity coefficient to the parameter Σ_x is defined as

$$S_{\Sigma_x}^{R} = \frac{dR(\Sigma_x)/R(\Sigma_x)}{d\Sigma_x/\Sigma_x} \tag{1}$$

For this study, R represents the whole core k_{eff} and Σ_x represents two-group macroscopic XSs. k_{eff} can be expressed as a ratio of two reaction rates integrated over some phase-space range such as

$$k_{eff} = \frac{\langle \phi^*, B\phi \rangle}{\langle \phi^*, A\phi \rangle} \tag{2}$$

The flux ϕ and adjoint flux ϕ^* are the solution of the diffusion equation for an eigenvalue problem and the generalized adjoint balance equation.

$$(A-\lambda B)\phi = L\phi = 0 \tag{3}$$

$$(A^*-\lambda B^*)\phi^* = L^*\phi^* = 0 \tag{4}$$

Where, A is the neutron loss operator and B is the fission neutron production operator. A^* is the adjoint neutron loss term and B^* is the adjoint production term.

As we know, $\lambda = 1/k_{eff}$. With use of this equation, one can obtain

$$\lambda = \frac{\langle \phi^*, A\phi \rangle}{\langle \phi^*, B\phi \rangle} \tag{5}$$

The relative change of λ in response to a first-order perturbation is given by Eq. (6).

$$\frac{d\lambda}{\lambda} = d(\ln(\lambda)) = \frac{\langle \phi^*, dA\phi \rangle}{\langle \phi^*, A\phi \rangle} - \frac{\langle \phi^*, dB\phi \rangle}{\langle \phi^*, B\phi \rangle} + \frac{\langle d\phi^*, A\phi \rangle}{\langle \phi^*, A\phi \rangle} - \frac{\langle d\phi^*, B\phi \rangle}{\langle \phi^*, B\phi \rangle} + \frac{\langle \phi^*, Ad\phi \rangle}{\langle \phi^*, A\phi \rangle} - \frac{\langle \phi^*, Bd\phi \rangle}{\langle \phi^*, B\phi \rangle} \tag{6}$$

According to the properties of adjoint operators as shown in the following equations,

$$\begin{aligned} \langle \phi^*, Ad\phi \rangle &= \langle d\phi, A^*\phi^* \rangle \\ \langle \phi^*, Bd\phi \rangle &= \langle d\phi, B^*\phi^* \rangle \end{aligned} \tag{7}$$

The Eq. (6) can be expressed as

$$\frac{d\lambda}{\lambda} = \frac{\langle \phi^*, dA\phi \rangle}{\langle \phi^*, A\phi \rangle} - \frac{\langle \phi^*, dB\phi \rangle}{\langle \phi^*, B\phi \rangle} + \langle d\phi, S^* \rangle + \langle d\phi^*, S \rangle \tag{8}$$

Where,

$$\begin{aligned} S &= \frac{A\phi}{\langle \phi^*, A\phi \rangle} - \frac{B\phi}{\langle \phi^*, B\phi \rangle} \\ S^* &= \frac{A^*\phi^*}{\langle \phi^*, A\phi \rangle} - \frac{B^*\phi^*}{\langle \phi^*, B\phi \rangle} \end{aligned} \tag{9}$$

A change in some input parameter appearing in the A and B operators will perturb the neutron balance and is mathematically compensated for by a change in the eigenvalue. The perturbed neutron balance equation is

$$(A+\Delta A)(\phi+\Delta\phi) = (\lambda+\Delta\lambda)(B+\Delta B)(\phi+\Delta\phi) \tag{10}$$

Neglecting terms involving products of perturbations in equation (10) gives a first-order approximation for the flux perturbation:

$$(A-\lambda B)d\Phi = -(dA - d(\lambda B))\Phi = -dL\Phi \tag{11}$$

Now we define the "generalized adjoint equation" and " generalized neutron equation " [17] as

$$(A-\lambda B)\Gamma = L\Gamma = S \tag{12}$$

$$(A^*-\lambda B^*)\Gamma^* = L^*\Gamma^* = S^* \tag{13}$$

The solutions, Γ , Γ^*, to these equations are called "generalized flux" and "generalized adjoint flux" respectively. Since

$$\langle d\phi, S^* \rangle = \langle d\phi, L^*\Gamma^* \rangle = \langle \Gamma^*, Ld\phi \rangle = -\langle \Gamma^*, dL\phi \rangle \tag{14}$$

$$\langle d\phi^*, S \rangle = \langle d\phi^*, L\Gamma \rangle = \langle \Gamma, L^*d\phi^* \rangle = -\langle \Gamma, dL^*\phi^* \rangle \tag{15}$$

$$\frac{d\lambda}{\lambda} = \frac{\langle \phi^*, dA\phi \rangle}{\langle \phi^*, A\phi \rangle} - \frac{\langle \phi^*, dB\phi \rangle}{\langle \phi^*, B\phi \rangle} - \langle \Gamma^*, dL\phi \rangle - \langle \Gamma, dL^*\phi^* \rangle \tag{16}$$

Then the Eq. (6) can be expressed as

Based on the definition of the generalized flux and generalized adjoint flux, they can be rewritten as

$$\Gamma = \frac{\Phi}{\lambda\left\langle \Phi^*, B\Phi \right\rangle} \qquad \Gamma^* = \frac{\Phi^*}{\lambda\left\langle \Phi^*, B\Phi \right\rangle} \tag{17}$$

According to the properties of adjoint operators, we can know that

$$\left\langle \Phi\delta L^*\Phi^* \right\rangle = \left\langle \Phi^*\delta L\Phi \right\rangle \tag{18}$$

And the following relation can be derived by taking account of $L = A - \lambda B$ (seen as Eq. (19):

$$\left.\begin{aligned} \delta L &= (\delta A - \lambda\delta B) - \delta\lambda B \\ (\delta A - \lambda\delta B) - 2\delta L &= \delta\lambda B - \delta L \end{aligned}\right\} \Rightarrow \delta\lambda B - \delta L = -(\delta A - \lambda\delta B) \tag{19}$$

Then the k_{eff} sensitivity coefficient to the parameter Σ_x can be expressed as

$$S_{\Sigma_x}^{k_{eff}} = -\frac{\Sigma_x}{k_{eff}} \frac{\left\langle \phi^* (\delta A - \frac{1}{k_{eff}}\delta B) \middle/ \delta\Sigma_x \phi \right\rangle}{\left\langle \phi^* \frac{1}{k_{eff}^2} B\phi \right\rangle} \tag{20}$$

For this study multi-group forward and adjoint flux solutions are directly calculated based on diffusion theory on the full core level. Then the effects of various perturbations can be estimated with equation (20), using the multi-group diffusion theory representation for the operators *A* and *B*. In numerical calculations, the space dependence of the variables is discretized, so that volume integrals become summations over mesh intervals. Table 2 shows k_{eff} sensitivity coefficient to various macroscopic XSs written out in detail.

Table 2 k_{eff} sensitivity coefficient to various macroscopic XSs based on diffusion theory

Sensitivity Coefficient	Numerator	Denominator
$S_{\Sigma_{a,g,z}}^{k_{eff}}$	$-k_{eff}\sum_{z=1}\Sigma_{a,g,z}\phi_{g,z}\phi_{g,z}^*V_z$	$\sum_{z=1}^{M}\sum_{g=1}^{G}\left[(\nu\Sigma_f)_{g,z}\phi_{g,z}^*\sum_{g'=1}^{G}(\chi_{g',z}\phi_{g',z})\right]V_z$
$S_{(\nu\Sigma_f)_{g,z}}^{k_{eff}}$	$(\nu\Sigma_f)_{g,z}\sum_{z=1}\phi_{g,z}\sum_{g'=1}^{G}(\chi_{g',z}\phi_{g',z}^*)V_z$	
$S_{\Sigma_{s,g-g',z}}^{k_{eff}}$	$-k_{eff}\Sigma_{s,g-g',z}\sum_{z=1}\phi_{g,z}(\phi_{g,z}^*-\phi_{g',z}^*)V_z$	
$S_{D_{g,z}}^{k_{eff}}$	$-\sum_{z=1}D_{g,z}\nabla\phi_{g,z}\nabla\phi_{g,z}^*V_z$	

4 Covariance matrix for few-group macroscopic XSs

Original multi-group microscopic XSs uncertainties are correlated, which can be described by a covariance matrix. These uncertainties propagate to all the assemblies in the core and these assemblies with same materials and similar spectra will be correlated. In this work, few-group macroscopic XSs uncertainties of all the 24 different types of assemblies are propagated from the same Scale's 44-group covariance matrix. So correlation inevitably exists between different macroscopic XSs of various assemblies and should be quantified. Taking account of the definition of covariance, the covariance between two different macroscopic XSs can be expressed as

$$\text{cov}(\Sigma_x, \Sigma_y) = \left\langle \delta\Sigma_x \delta\Sigma_y \right\rangle \tag{21}$$

where, $\delta\Sigma_x$, $\delta\Sigma_x$ represent difference between the values and expectations of the few-group macroscopic XSs. < > represents integration over the ranges of Σ_x , Σ_y with their probability density functions.

Using the linear approximation, one can show

that the difference between the macroscopic XS value and expectation due to a small perturbation in an energy-dependent microscopic cross section σ_i can be expressed as

$$\delta\Sigma_x = \sum_{i=1}^{n} \frac{\partial \Sigma_x}{\partial \sigma_i}\delta\sigma_i$$
$$\delta\Sigma_y = \sum_{j=1}^{n} \frac{\partial \Sigma_y}{\partial \sigma_j}\delta\sigma_j \quad (22)$$

Here n is number of energy group. $\delta\sigma_i$, $\delta\sigma_j$ represent the difference between the values and expectations of the multi-group microscopic XSs. With use of the Eq. (21), one can obtain

$$\frac{\mathrm{cov}(\Sigma_x,\Sigma_y)}{\Sigma_x\Sigma_y} = \left\langle \sum_{i=1}^{n}\frac{\partial\Sigma_x}{\partial\sigma_i}\delta\sigma_i \sum_{j=1}^{n}\frac{\partial\Sigma_y}{\partial\sigma_j}\delta\sigma_j \frac{1}{\Sigma_x}\frac{1}{\Sigma_y}\right\rangle \quad (23)$$
$$= \left\langle \sum_{i=1}^{n}\sum_{j=1}^{n}\frac{\partial\Sigma_x/\Sigma_x}{\partial\sigma_i/\sigma_i}\frac{\partial\Sigma_y/\Sigma_y}{\partial\sigma_j/\sigma_j}\frac{\delta\sigma_i\delta\sigma_j}{\sigma_i\sigma_j}\right\rangle$$

$$S_{\sigma_i}^{\Sigma_x} = \frac{\partial\Sigma_x/\Sigma_x}{\partial\sigma_i/\sigma_i}$$
$$S_{\sigma_j}^{\Sigma_y} = \frac{\partial\Sigma_y/\Sigma_y}{\partial\sigma_j/\sigma_j} \quad (24)$$

Where, The Σ_x, Σ_y sensitivity coefficient to the parameters σ_i, σ_j are represented as Eq.(24),
which are directly calculated by using Tsunami-2D module based on GPT in this work [18]. So the relative covariance between different macroscopic XSs can be expressed as

$$RCov(\Sigma_x,\Sigma_y) = \frac{\mathrm{cov}(\Sigma_x,\Sigma_y)}{\Sigma_x\Sigma_y}$$
$$= \sum_{i=1}^{n}\sum_{j=1}^{n} S_{\sigma_i}^{\Sigma_x} S_{\sigma_j}^{\Sigma_y} RCov(\sigma_i,\sigma_j) \quad (25)$$

In this work, $RCov(\sigma_i,\sigma_j)$ is the Scale's 44-group relative covariance matrix.

Based on the sensitivity information and original relative covariance matrix, all the relative covariance between different macroscopic XSs of various assemblies can be quantified according to Eq. (25). Particularly, the correlation coefficient is equal to 1 for the same macroscopic XS of the same type of assembly, which means fully correlated. Then the few-group macroscopic XSs covariance matrix for the full-core denoted as C_{core} can be constructed according to the arrangement of assemblies in the core, as shown in the Fig.4.

Where, the resulting C_{core} matrix is of dimension $I \times I$ and $I = N \times 7$. N is the total number of assemblies in the core model and 7 represents Σ_{a1}, Σ_{a2}, $\upsilon\Sigma_{f1}$, $\upsilon\Sigma_{f2}$, Σ_{s1-2}, D_1, D_2 in this study, which will be directly used to whole core diffusion calculation and k_{eff} uncertainty analysis. Especially that the diffusion coefficient is defined as

$$D = \frac{1}{3\left[(1-2/3A)\Sigma_s - \Sigma_a\right]} \quad (26)$$

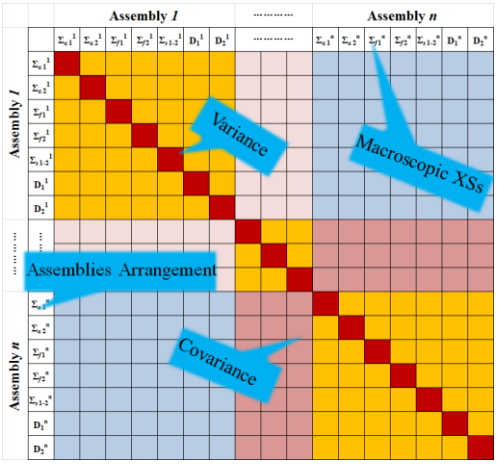

Fig. 4 Few-group macroscopic XSs covariance matrix arrangement for the full-core.

Here A is the nuclear mass number.
As for the whole core few-group macroscopic XSs covariance matrix C_{core}, the diagonal elements are the relative variance values for each of the macroscopic XSs. That is to say the square root of each diagonal element is the uncertainty of each macroscopic XS. And the off-diagonal elements are the relative covariance between different macroscopic XSs.

Based on k_{eff} sensitivity coefficients to different few-group macroscopic XSs of all assemblies in the core and the corresponding few-group macroscopic XSs covariance matrix for the whole core, the uncertainty of

core k_{eff} propagated from nuclear data can be quantified as

$$\sigma(k_{eff}) = \sqrt{S_{\Sigma}^{k_{eff}} C_{core} S_{\Sigma}^{k_{eff}\,T}} \tag{27}$$

5 Numerical verification and results

5.1 Verification of k_{eff} sensitivity coefficient calculations using GPT and diffusion theory

For this study the validity of the total sensitivity coefficients is confirmed through the use of the direct perturbation (DP) sensitivity calculation. The direct perturbation sensitivity coefficient of k_{eff} to some macroscopic cross section Σ_x is computed as

$$S_{\Sigma_x}^{k_{eff}} = \frac{dk_{eff}/k_{eff}}{d\Sigma_x/\Sigma_x} = \frac{\Sigma_x}{k_{eff}} \times \frac{k_{eff}^{\Sigma_x^+} - k_{eff}^{\Sigma_x^-}}{\Sigma_x^+ - \Sigma_x^-} \tag{28}$$

where Σ_x^+ and Σ_x^- represent the increased and decreased values of some macroscopic cross section by a certain percentage and $k_{eff}^{\Sigma_x^+}$ and $k_{eff}^{\Sigma_x^-}$ represent the corresponding values of k_{eff}. The use of DP calculations to confirm the validity of sensitivity coefficients is strongly encouraged.

In this study, each macroscopic cross section was perturbed by ±1% and the whole core diffusion calculation was repeated by using CITATION code. Then the direct perturbation sensitivity coefficients were computed by using the k_{eff} values from the unperturbed and perturbed cases in Eq. (28). To demonstrate the importance of assembly discontinuity factor (ADF) in adjusting the accuracy of sensitivity coefficients calculated by GPT on the core level, the model as shown in Fig.2 was run respectively with or without considering ADFs between different assemblies. The results are given in Table 3, where DP represents k_{eff} sensitivity coefficients to macroscopic XSs are computed by direct perturbation method and GPTCD represents generalized perturbation theory coupled diffusion calculation. W/o or w ADF represents diffusion calculation without or with considering assembly discontinuity factor adjustment.

Table 3 Comparison of k_{eff} sensitivity coefficients from different methods for mini-core

Macro-XS	DP w/o ADF	GPTCD w/o ADF	RE/%	DP w ADF	GPTCD w ADF	RE/%
Σ_{a1}	-3.47392E-01	-3.42512E-01	-1.40	-3.47038E-01	-3.42255E-01	-1.38
Σ_{a2}	-7.77804E-01	-7.71400E-01	-0.82	-7.78432E-01	-7.71414E-01	-0.90
$\nu\Sigma_{f1}$	2.13168E-01	2.13224E-01	0.03	2.12959E-01	2.12984E-01	0.01
$\nu\Sigma_{f2}$	7.86553E-01	7.86775E-01	0.03	7.86351E-01	7.87022E-01	0.09
$\Sigma_{s,1\text{-}2}$	1.47149E-01	1.45503E-01	-1.12	1.45865E-01	1.45377E-01	-0.33
D_1	-1.28259E-02	-1.21703E-02	-5.11	-1.29479E-02	-1.21695E-02	-6.01
D_2	-1.69020E-03	-1.36122E-03	-19.46	-1.35140E-03	-1.39864E-03	3.50

According to the results in Table 3, the sensitivity coefficient results using ADF adjustment show good agreement with the direct perturbation results for all macroscopic cross sections. Due to omission of ADF between different assemblies, the results do not show good agreement with the direct perturbation results, especially for k_{eff} sensitivity coefficient to scattering cross-section and diffusion coefficients.

This is because flux gradient in $S_{\Sigma_{s,g-g',z}}^{k_{eff}}$ and $S_{D_{g,z}}^{k_{eff}}$, as shown in Table 2, cannot be computed correctly using diffusion theory without considering assembly discontinuity factors.

The maximum difference between GPTCD

w/o ADF results and the direct perturbation results occurs for thermal diffusion coefficient with a magnitude of 19.46%. Although the maximum difference between GPTCD w ADF results and the direct perturbation results occurs for fast diffusion coefficient with a magnitude of 6.01%, the k_{eff} sensitivity coefficient to diffusion coefficients is very small, as shown in Fig.5. Thus, the use of generalized perturbation theory coupled with diffusion calculation with assembly discontinuity factor adjustment to computer sensitivity coefficients is recommended and the results agree well with the direct perturbation results.

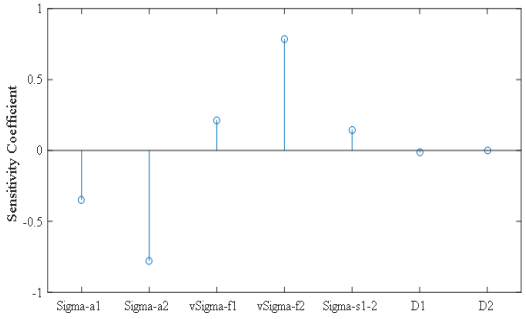

Fig. 5 The total k_{eff} sensitivity coefficients to different macroscopic XSs.

5.2 Verification of k_{eff} uncertainty quantified by using GPT and diffusion theory

In order to confirm the validity of uncertainty quantification method, Tsunami-3d-k5 module in Scale 6.1 is applied to perform uncertainty analysis of the same mini-core model shown in Fig.2. For Tsunami-3d-k5, the uncertainty in the calculated value of k_{eff} is directly estimated from energy -dependent multi-group microscopic cross-section-covariance matrices. While the uncertainty in k_{eff} quantified GPTCD method is estimated from homogenized two-group cross-section-covariance matrices. For the purpose to explain the importance of the correlation coefficients between two macroscopic cross-sections, two k_{eff} uncertainty quantification cases are designed in this study. Where, the case of GPTCD w/o Cov represents that the uncertainty in k_{eff} is quantified by using GPTCD method without correlation coefficients between different macroscopic XSs taken into account. And GPTCD w/o A-Cov denotes that correlation coefficients between macroscopic cross-sections in different assemblies are not considered while those between macroscopic XSs in the same assembly are considered. The uncertainties in k_{eff} quantified from different covariance matrices are compared and shown in Table 4.

Table 4 Comparison of k_{eff} uncertainty quantified from different covariance matrix(%Δk/k)

Rod position/cm	Tsunami-3d-k5	GPTCD w/o Cov [a]	GPTCD w/o A-Cov [b]
0	0.5341±0.00072	0.18923	0.17650
96	0.5285±0.00066	0.18139	0.16881
320	0.5215±0.00070	0.19797	0.18115

Observation of the results in Table 4 shows that the uncertainty in k_{eff} propagated from nuclear data is very small compared with the Tsunami-3d-k5 results. The uncertainty in k_{eff} is about 0.0053 with the correlation taken into account while it is about 0.0018 without. Thus the correlation effect of the two-group cross sections of different assemblies on the core k_{eff} is estimated to be roughly 350pcm and there will be a slight variations in the effect with the movement of control rod. For the reason that the correlation between different macroscopic cross-sections should be quantified accurately. Based on the method studied in the work, the homogenized two-group cross-section-covariance matrix for the mini-core was constructed for further uncertainty analysis, as shown in Fig. 6.

In the previous section, it has been proven that the sensitivity coefficients calculation method and the homogenized two-group cross-section-covariance matrix constructed in this work are correct. Then the uncertainty in the core k_{eff} can be quantified by using the k_{eff}

sensitivity coefficients to different macroscopic cross-sections and the corresponding covariance matrix as shown in Eq. (27). The relative uncertainties in k_{eff} for the mini-core with varying insertion depths of control rod quantified by different methods are compared and shown in Table 5. Where, the DP means that the uncertainty in k_{eff} was quantified by using the direct perturbation sensitivity coefficients and SS represents that statistical sampling method was used to quantify k_{eff} uncertainty propagated from macroscopic XSs. The difference between uncertainties quantified by DP method and Tsunami-3d-k5 mainly derives from the newly introduced uncertainties in the construction of the homogenized two-group cross-section-covariance matrix. Thus the effect of constructing two-group cross-section-covariance matrix from the evaluated covariance matrices on the k_{eff} uncertainty is estimated to be less than 100pcm. Observation of results in Table 5 shows that the uncertainty of k_{eff} from DP, SS and GPTCD w ADF methods are roughly similar, which indicates that the nuclear data uncertainties propagation and quantification method based on generalized perturbation theory coupled with diffusion calculation with ADFs taken into account on whole core level is correct. The total uncertainty of k_{eff} for the mini-core propagated from uncertainties in nuclear data is about 0.52%, which is significant to neutronics calculations.

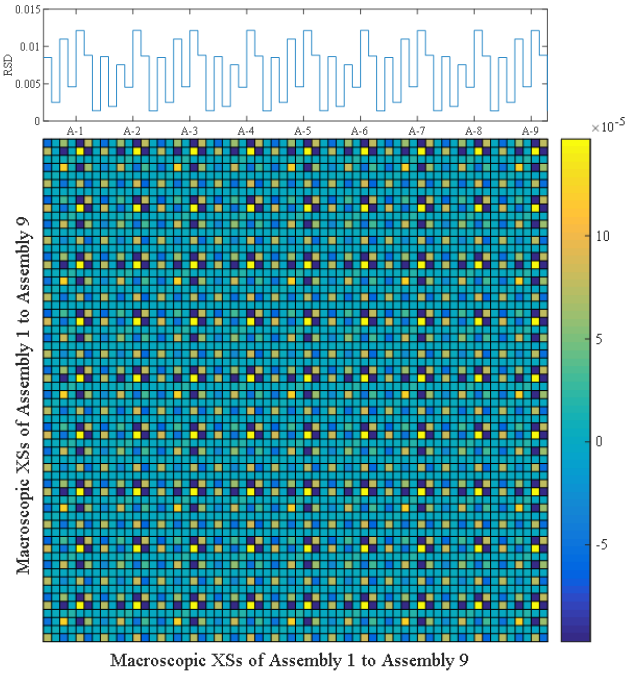

Fig. 6 Homogenised two-group macroscopic XSs covariance matrix for Mini-core without CR.

Table 5 Comparison of k_{eff} uncertainty quantified by different methods for mini-core

Rod position/cm	%Δk/k			
	Tsunami-3d-k5	DP	GPTCD w ADF	SS [a]
0	0.5341±0.00072	0.5237	0.52439	0.5273±0.00038
96	0.5285±0.00066	0.52283	0.52359	0.5264±0.00038
320	0.5215±0.00070	0.52295	0.52335	0.5238±0.00037

5.3 Sensitivity and uncertainty analysis for k_{eff} of AP1000 core

The information for AP1000 core model is given in section2.1. Only fresh fuel assemblies are considered in this study. Uncertainty in k_{eff} propagated from homogenized two-group cross sections is analyzed at Hot Zero Power (HZP) condition as well as Hot Full Power (HFP) condition. Information for these operating conditions is available in Table 6.

Table 6 AP1000 core operating conditions [19]

Case	HZP	HFP
Fuel temperature (K)	565	900
Cladding temperature(K)	565	600
Moderator temperature(K)	565	585
Density of moderator(g/cc)	0.743	0.661
Fuel density(g/cc)	10.476	10.476
Reactor system pressure(psi)	2250	2250
Reactor Power(MW)	3.411	3411

Table 7 presents the k_{eff} values and the corresponding uncertainties that were quantified by different methods at HZP and HFP. At the same time, the uncertainty of k_{eff} can be also predicted by applying SS method based on the relative two-group homogenized cross-section-covariance matrices. In this study, 100 is selected as the size for each sample and the mean value and uncertainty of k_{eff} with their errors is given in Table 7. Where, k_{eff} is 0.96179 ± 0.48445 at HZP condition and 0.94899 ± 0.53248 at HFP condition quantified by GPTCD w ADF method, while it is 0.962382 ± 0.49944 by SS method. Observations of the results in Table 7 shows that uncertainty in k_{eff} rises as the temperature increases but the k_{eff} itself has an opposite tendency towards temperature. This is due to the effect of Doppler broadening and the reduction of neutron moderation in the core because of reducing moderator density.

Table 7 k_{eff} uncertainty for AP1000 core at HZP and HFP

Condition	GPTCD w ADF		SS method	
	k_{eff}	%Δk/k	k_{eff}	%Δk/k
HZP	0.96179	0.48445	0.962382 ± 0.00051	0.49944 ± 0.00038
HFP	0.94899	0.53248	--	--

The contributions of individual two-group cross-section covariance matrices to the uncertainty of k_{eff} are shown in Table 8. The relative uncertainty of k_{eff} can be calculated from individual values by adding the square of the values with positive signs and subtracting the square of the values with negative signs, then taking the square root. Table 8 shows that the largest contributor to the uncertainty in k_{eff} is due to $\nu\Sigma_{f2}$, which is followed by Σ_{a1} and $\Sigma_{s,1\text{-}2}$. This is because of large uncertainty in $\nu\Sigma_{f2}$ and high sensitivity to k_{eff}. It can be also seen from Table 8 that contributions to the uncertainty in k_{eff} due to homogenized cross-section-covariance rises from HZP condition to HFP condition, and a same tendency occurs in the k_{eff} sensitivity to fast group lattice-averaged cross-section but an opposite trend in thermal cross-sections , as shown in Fig.7 to Fig.13. This is due to the effect of hardening of neutron spectrum as the temperature rises and the reduction of neutron moderation.

Table 8 Contributions to uncertainty in k_{eff} by individual macroscopic XS covariance matrices

Covariance Matrices		Contributions to uncertainty in k_{eff} (%Δk/k)	
Macroscopic XS	Macroscopic XS	HZP	HFP
Σ_{a1}	Σ_{a1}	2.8855E-03	3.4068E-03
Σ_{a1}	Σ_{a2}	1.4090E-03	1.4705E-03
Σ_{a1}	$\nu\Sigma_{f1}$	2.1587E-03	2.5207E-03
Σ_{a1}	$\nu\Sigma_{f2}$	4.5963E-04	6.5957E-04
Σ_{a1}	$\Sigma_{s,1\text{-}2}$	-3.0924E-03	-3.6972E-03
Σ_{a1}	D_1	-1.1136E-03	-1.3457E-03
Σ_{a1}	D_2	9.0244E-06	6.2167E-06
Σ_{a2}	Σ_{a2}	1.6512E-03	1.7664E-03
Σ_{a2}	$\nu\Sigma_{f1}$	-4.2596E-04	-4.3833E-04
Σ_{a2}	$\nu\Sigma_{f2}$	-1.6831E-03	-1.8038E-03
Σ_{a2}	$\Sigma_{s,1\text{-}2}$	6.4643E-04	7.5643E-04
Σ_{a2}	D_1	7.4029E-05	9.8631E-05
Σ_{a2}	D_2	-3.6690E-05	-4.3632E-05
$\nu\Sigma_{f1}$	$\nu\Sigma_{f1}$	1.7781E-03	2.0342E-03
$\nu\Sigma_{f1}$	$\nu\Sigma_{f2}$	1.5723E-03	1.7418E-03
$\nu\Sigma_{f1}$	$\Sigma_{s,1\text{-}2}$	-2.1478E-03	-2.4052E-03
$\nu\Sigma_{f1}$	D_1	-6.4014E-04	-8.1106E-04
$\nu\Sigma_{f1}$	D_2	-1.4049E-05	-1.7304E-05
$\nu\Sigma_{f2}$	$\nu\Sigma_{f2}$	3.4690E-03	3.6574E-03
$\nu\Sigma_{f2}$	$\Sigma_{s,1\text{-}2}$	2.5742E-04	2.7823E-04
$\nu\Sigma_{f2}$	D_1	8.1446E-05	2.2606E-04
$\nu\Sigma_{f2}$	D_2	4.0461E-05	4.6965E-05
$\Sigma_{s,1\text{-}2}$	$\Sigma_{s,1\text{-}2}$	2.2444E-03	2.6510E-03
$\Sigma_{s,1\text{-}2}$	D_1	1.0566E-03	1.2783E-03
$\Sigma_{s,1\text{-}2}$	D_2	3.1627E-05	3.2566E-05
D_1	D_1	2.8439E-04	3.5090E-04
D_1	D_2	1.1087E-05	1.4006E-05
D_2	D_2	4.5919E-06	6.1844E-06

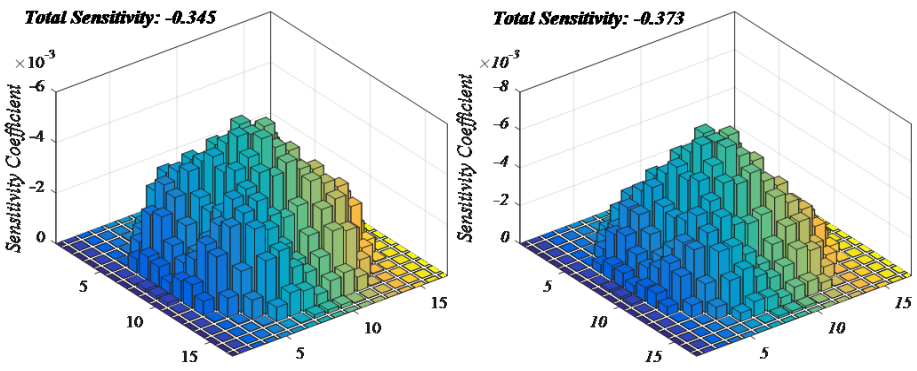

Fig. 7 k_{eff} sensitivity coefficient to Σ_{a1} of different assemblies at HZP(left) and HFP(right).

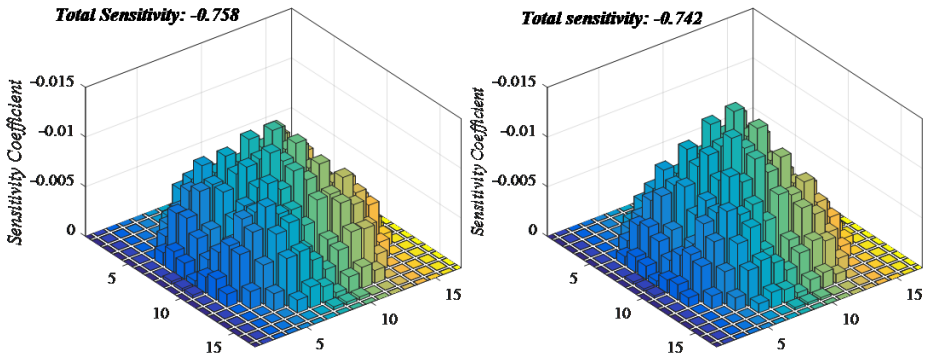

Fig. 8 k_{eff} sensitivity coefficient to Σ_{a2} of different assemblies at HZP(left) and HFP(right).

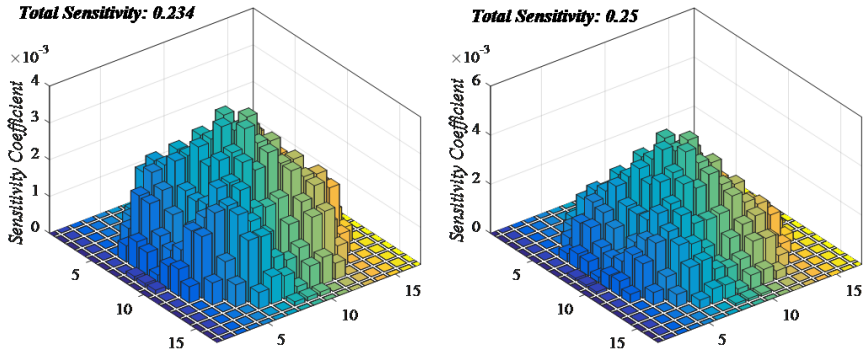

Fig. 9 k_{eff} sensitivity coefficient to $\nu\Sigma_{f1}$ of different assemblies at HZP(left) and HFP(right).

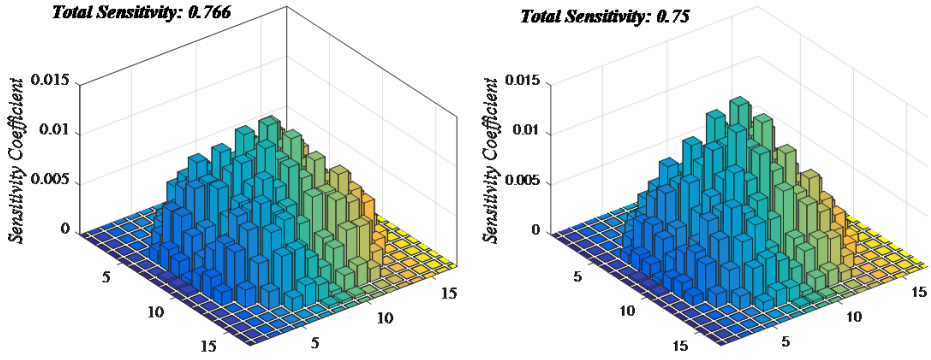

Fig. 10 k_{eff} sensitivity coefficient to $\nu\Sigma_{f2}$ of different assemblies at HZP(left) and HFP(right).

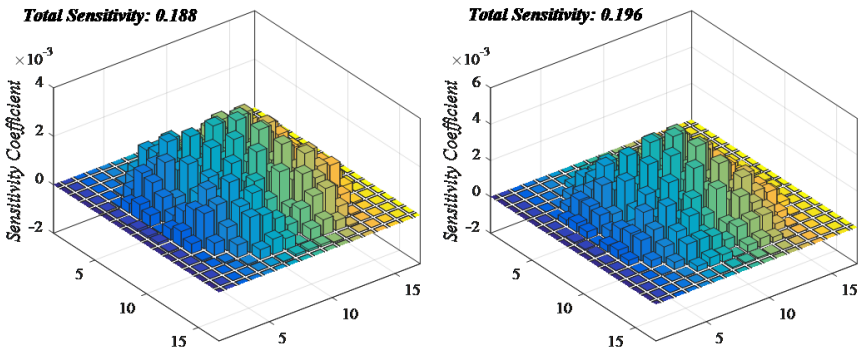

Fig. 11 k_{eff} sensitivity coefficient to Σ_{s1-2} of different assemblies at HZP(left) and HFP(right).

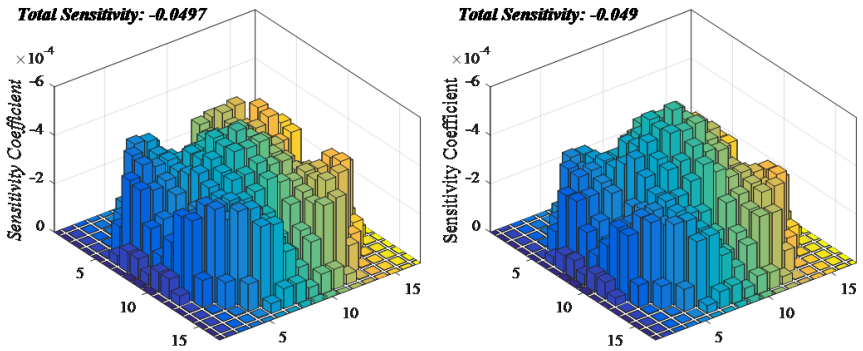

Fig. 12 k_{eff} sensitivity coefficient to D_1 of different assemblies at HZP(left) and HFP(right).

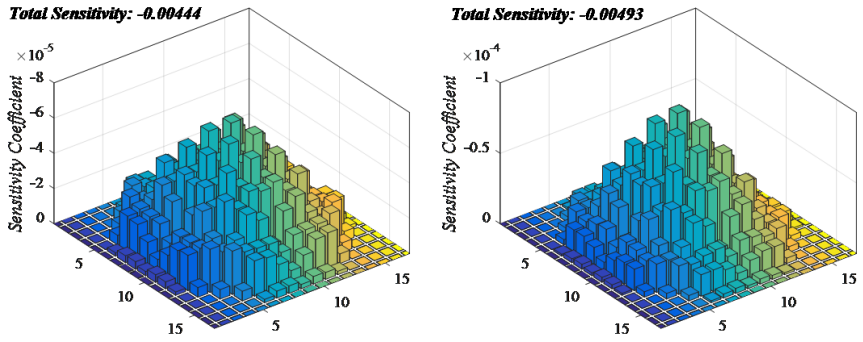

Fig. 13 k_{eff} sensitivity coefficient to D_2 of different assemblies at HZP(left) and HFP(right).

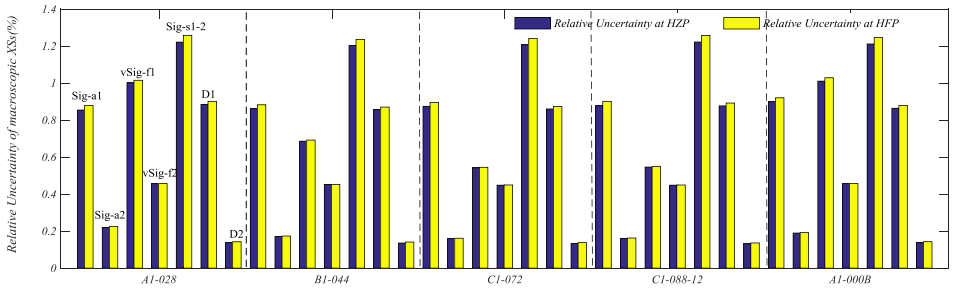

Fig. 14 Relative uncertainties of macroscopic XSs of different assemblies at HZP and HFP.

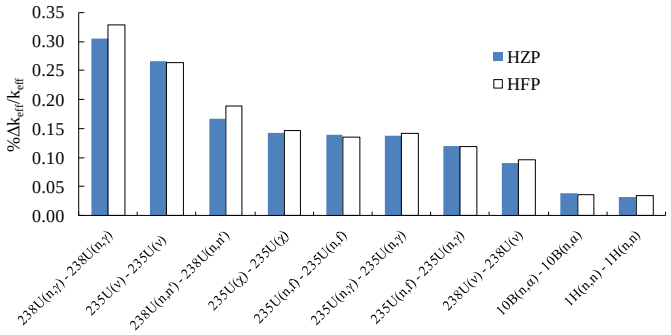

Fig. 15 The top ten contributors to the uncertainty in k_{eff} at HZP and HFP.

Another reason for the uncertainty in k_{eff} rises as the temperature increases is that the uncertainty in two-group macroscopic cross-sections propagated from multi-group microscopic cross-sections increases with increasing temperature, as shown in Fig.14. Based on the previous study, we know that the largest contributor to the uncertainty in k_{eff} is due to ^{238}U (n,γ) reaction, as shown in Fig.15. The majority of neutron capture reaction in ^{238}U occurs at the intermediate energy and the neutron spectrum shifts into the epithermal range, *i.e.* increasing temperature leads a harder neutron spectrum when changing from HZP to HFP conditions. At the same time, the uncertainties in ^{238}U (n,γ) and ^{238}U (n,n') reactions are much larger than those in ^{235}U(ν) although k_{eff} is most sensitive to ^{235}U(ν) reaction. So the uncertainty in k_{eff} increases when changing from HZP to HFP conditions. It can be also seen from Fig.14 that uncertainties in the fast group cross-sections are much larger than those in the thermal group cross-sections.

As analyzed above, the total relative uncertainty in k_{eff} of AP1000 core propagated from nuclear data is about 0.5% and this value will increase as the temperature rises.

6 Conclusion

The motivation of this presented work is to study new strategy for quantifying and propagating nuclear data uncertainty on the core level by using generalized perturbation theory coupled with diffusion calculation. The k_{eff} sensitivity coefficients to homogenized few-group cross-sections have been derived by applying generalized perturbation theory based on diffusion calculation results. Most importantly, the covariance between the homogenized few-group cross-sections of all the possible pairings of fuel assemblies comprising the core must be estimated accurately. Therefore, a method of correlation analysis between different few-group XSs based on sensitivity information has been studied in depth to construct few-group homogenized cross-section-covariance matrices for uncertainty analysis on the core level.

The direct perturbation sensitivity coefficient calculation method and uncertainty results from Tsunami-3d-k5 for the mini-core model has been used to confirm the validity of sensitivity and uncertainty analysis methods studied in this work and the numerical results indicate that the generalized perturbation theory coupled with diffusion calculation with assembly discontinuity factor adjustment method is recommended to quantify sensitivity coefficients and the few-group cross-section-covariance matrices can be used for uncertainty analysis on the core level.

The uncertainties of k_{eff} of the traditional first core of the advanced commercial power reactor AP1000 at the hot zero power (HZP) state and hot full power (HFP) state has been quantified and some important conclusions can be obtained from the numerical results: (i)the uncertainty of k_{eff} of AP1000 core due to

uncertainties in nuclear cross sections is about 0.5%, which is significant to nuclear reactor physics calculation; (ii) Increasing temperature leads to increasing uncertainty in k_{eff} which is mainly affected by hardening of neutron spectrum.

In the future work, the correlation analysis between k_{eff} of different core conditions, especially with varying insertion depths of control rod, will be studied in-depth. Based on these correlation information and uncertainty information of k_{eff} quantified in this paper, the uncertainty of control rod worth due to uncertainty in nuclear data can be quantified.

Acknowledgments

This work is supported by the Chinese National Natural Science Foundation Project 11505038 and Young Elite Scientists Sponsorship Program by CAST.

Reference

[1] IVANOV, K., and AVRAMOVA, M., *et al.*: Benchmarks for uncertainty analysis in modeling (UAM) for the design, operation and safety analysis of LWRs. OECD/NEA, NEA/NSC/ DOC (2013) 7, 2013.

[2] MPACT Team: MPACT Theory Manual, Version 1.0. University of Michigan, Ann Arbor, MI, USA, 2013.

[3] REITSMA, F., and STRYDOM, G., *et al.*: The IAEA coordinated research program on HTGR reactor physics, thermal-hydraulics and depletion uncertainty analysis: description of the benchmark test cases and phases. Proceeding of the HTR 2012 Tokyo, Japan, October 28-November 1, 2012.

[4] BRATTON, R.N., AVRAMOVA, M., and IVANOV, K.: OECD/NEA Benchmark for Uncertainty Analysis in Modeling(UAM) for LWRS-Summary and Discussion of Neutronics cases (phase I). Nuclear Engineering and Technology, 2014, 46(3):313-342.

[5] HAO, C., ZHAO, Q., and LI, F., *et al.*: Uncertainty Analysis of Advanced Pressurized Water Reactor Fuel Assembly. Nuclear Power Engineering, 2016,37(3): 173-180.

[6] ARENAS, C., BRATTON, R., and REVENTOS, F., *et al.*: Uncertainty analysis of light water reactor fuel lattices. Science and Technology of Nuclear Installations, v2013, article ID 437409, 10 pages.

[7] SCALE: A Comprehensive Modeling and Simulation Suite for Nuclear Safety Analysis and Design. Radiations Safety Information Computational Center. Oak Ridge National Laboratory, ONRL/TM-2005/39, 2011.

[8] PUSA, M.: Incorporating Sensitivity and Uncertainty Analysis to a Lattice Physics Code with Application to CASMO-4. Annals of Nuclear Energy, 2012, 40: 153-162.

[9] AUGUSTO, H.S., CHRISTOPHE, D., and CHRISTIAN, E.: Uncertainty and sensitivity analyses applied to the DRAGONv4.05 code lattice calculations and based on JENDL-4 data. Annals of Nuclear Energy, 2013, 57: 230-245.

[10] REARDEN, B.T., and TSUNAMI -3D: Control Module for Three-Dimensional Cross-Section Sensitivity and Uncertainty Analysis for Criticality, Sect. C9 in SCALE: A Modular Code System for Performing Standardized Computer Analyses for Licensing Evaluations, ORNL/TM-2005/39, Version 6.1, Oak Ridge National Laboratory,2011.

[11] ARTEM, Y., BENJAMIN, C., and MARKUS, K. *et al.*: A two-step approach to uncertainty quantification of core simulators. Science and Technology of Nuclear Installations, v2012, 2012.

[12] HO, J.P., DONG, H., *et al.*: Uncertainty Propagation Analysis for Yonggwang Nuclear Unit 4 by MCCARD/MASTER Core Analysis System. Nuclear Engineering and Technology, 2014 46(3): 291-298.

[13] KLEIN, M., GALLNER, L., and KRZYKACZ-HAUSMANN, B., *et al.*: Influence of nuclear data uncertainties on reactor core calculations. Kerntechnik, 2011, 76(3):174-178.

[14] JESSEE, M.A., DEHART, M.D., and TRITON: A Multipurpose Transport, Depletion, and Sensitivity and Uncertainty Analysis Module, Sect. T1 in SCALE: A Modular Code System for Performing Standardized Computer Analyses for Licensing Evaluations, ORNL/TM-2005/39, Version 6.1, Oak Ridge National Laboratory,2011.

[15] LI, F., HU, Y., and LUO, Z.: Discontinuity-Factor Theory and Its Realization on Diffusion-Difference Equation. Nuclear Power Engineering, v16, p.115, 1995. (in Chinese)

[16] VONDY, D.R., CUNNINGHAM, G.W., FOWLER, T.B.: Nuclear Reactor Core Analysis: CITATION, Report ORNL-TM-2496, Rev.2, 1971.

[17] WILLIAMS, M.L.: Perturbation theory for nuclear reactor analysis. CRC Handbook of Nuclear Reactors Calculations, 1986, 3: 63-188.

[18] JESSEE, M.A., WILLIAMS, M.L., and DEHART, M.D.: Development of generalized perturbation theory capability within the SCALE code package. 2009 International Conference on Mathematics, Computational Methods & Reactor Physics (M&C 2009), Saratoga Springs, NY, 2009.

[19] GODFREY, A.T.: "VERA core physics benchmark progression problem specifications ". revision4, CASL-U-2012-0131-004, CASL, August, 2014. http://www.casl.gov/docs/CASL-U-2012-0131-004.pdf.